DiffSDS: A geometric sequence diffusion model for protein backbone inpainting

Anonymous authors
Paper under double-blind review

Abstract

Can a pure transformer learn protein structure under geometric constraints? Recent research has simplified protein structures as sequences of folding angles, making transformers suitable for unconstrained protein backbone generation. Unfortunately, such simplification is unsuitable for the constrained protein inpainting problem: we reveal theoretically that applying geometric constraints to the angle space would result in gradient vanishing or exploding, called **GradCurse**. As a remedy, we suggest adding a hidden **a**tomic **d**irection **s**pace (**ADS**) layer upon the transformer encoder, converting invariant backbone angles into equivariant direction vectors. Geometric constraints could be efficiently imposed on the direction space while avoiding GradCurse. Meanwhile, a Direct2Seq decoder with mathematical guarantees is also introduced to reconstruct the folding angles. We apply the **dual-space** model as the denoising neural network during the conditional diffusion process, resulting in a constrained generative model–**DiffSDS**. Extensive experiments show that the proposed DiffSDS outperforms the sequence diffusion baseline, and even achieves competitive results with coordinate diffusion models, filling the gap between sequence and coordinate diffusion models.

1 Introduction

We aim to **improve** and **simplify** the modeling of constrained protein backbone inpainting, i.e., recovering masked protein backbones, which has wide applications in *de-novo* protein design (Wang et al., 2022a; Lee & Kim, 2022; Ferruz et al., 2022). Existing protein structural generative models explicitly consider the equivariance caused by rotation and translation (Wang et al., 2022a; Trippe et al., 2022; Luo et al.; Anand & Achim, 2022). These considerations enable them to correctly consider atom interactions in the 3D space while requiring special model designs that increase the modeling complexity caused by 3D operations. Restricted by this, traditional powerful models, such as visual CNNs or sequence transformers, are prevented from being directly applied to structure modeling. Given the success of sequence transformers that seem to unify everything in NLP and CV, we wonder whether we can simplify protein backbone inpainting by treating it as a sequence modeling task. In this regard, the recent FoldingDiff (Wu et al., 2022a) suggests converting protein structures into sequences of folding angles, allowing transformers for unconditional protein backbone generation.

Unfortunately, the pure sequence model is unsuitable for constrained structure design tasks. In protein backbone inpainting, the designed structure should fit multiple geometric constraints, including linking the masked structure's endpoints and not overlapping with unmasked structures to meet the repulsion (Spassov et al., 2007; Müller-Späth et al., 2010; Drake & Pettitt, 2020). As shown in Fig.1, if the constraints are not guaranteed, specifically when the masked endpoints s and e are not connected, the generated structure will be meaningless. Unfortunately, we empirically find and theoretically prove that the imposing geometric constraints on the angle space generally lead to gradient explosion or vanishing called **GradCurse**. An open research question is how to efficiently and effectively impose geometric constraints on the sequence model while keeping its simplicity.

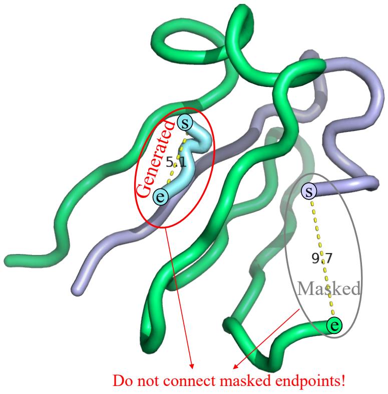

Figure 1: Violation of geometric constraints. Atoms between s and e are masked and should be recovered by the algorithm.

We suggest inserting a hidden **a**tomic **d**irection **s**pace (**ADS**) into the sequence model, allowing to impose structural constraints on the novel direction space efficiently. ADS is a plug-and-play cross-modal conversion technique connecting the sequence and direction space. By adding ADS upon the last transformer layer, we obtain the Seq2Direct encoder ($\mathrm{Enc}_{\mathrm{s2d}}$) that converts sequential features into direction vectors. We also introduce Direct2Seq decoder ($\mathrm{Dec}_{\mathrm{d2s}}$) according to strict mathematical transformations. A sequence model (SDS) equipped with hidden direction space could be constructed by stacking $\mathrm{Enc}_{\mathrm{s2d}}$ and $\mathrm{Dec}_{\mathrm{d2s}}$. SDS takes angular sequences as inputs and outputs, with a latent direction space that supports efficient geometric calculations and is mathematically consistent with the sequence space. In this design, multimodal constraints, e.g., sequential and 3D constraints, can be simultaneously considered on the corresponding feature space. Finally, we apply the SDS model as the denoising neural network during the conditional diffusion process, resulting in a constrained generative model–DiffSDS.

We evaluated DiffSDS on CATH4.3 and compared it with recent strong baselines, including RFDesign (Wang et al., 2022a), modified FoldingDiff (Wu et al., 2022a), SMCDiff Trippe et al. (2022), and RFDiffusion Watson et al. (2023). We also propose three metrics to evaluate the results of protein backbone inpainting, including protein likeness, connectivity, and non-overlapping. Experiments show that our methods significantly outperform baselines in all metrics. In addition, the designability of structures generated by DiffSDS is also better than baselines. As to simplicity, the proposed DiffSDS utilizes the sequence transformer to model protein structures, avoiding the equivariance consideration and GradCurse. We have also performed ablation studies to reveal the role of conditions and constraints.

1.1 Related Work

Problem Definition. Protein backbone inpainting aims to recover the continuous masked substructure of the protein backbone, given the unmasked atoms as conditions. The generated structure is required to connect different protein fragments with fixed spatial positions. Formally, we write the protein backbone as $\mathcal{B} = \{\boldsymbol{p}_1^C, \boldsymbol{p}_1^A, \boldsymbol{p}_1^N, \boldsymbol{p}_2^C, \boldsymbol{p}_2^A, \boldsymbol{p}_2^N, \cdots, \boldsymbol{p}_n^C, \boldsymbol{p}_n^A, \boldsymbol{p}_n^N\}$, where $\{\boldsymbol{p}_i^C, \boldsymbol{p}_i^A, \boldsymbol{p}_i^N\}$ indicates the set of backbone atoms (C, C_α and N) of the i-th residue and $\boldsymbol{p}_i^A$ is the 3D position of the i-th C_α. Denote the masked sub-structure as $\mathcal{M} = \{\boldsymbol{p}_i^C, \boldsymbol{p}_i^A, \boldsymbol{p}_i^N\}_{i=s}^{e}$, the unmasked structures as $\mathcal{K} = \{\boldsymbol{p}_i^C, \boldsymbol{p}_i^A, \boldsymbol{p}_i^N\}_{i=1}^{s-1} \cup \{\boldsymbol{p}_i^C, \boldsymbol{p}_i^A, \boldsymbol{p}_i^N\}_{i=e+1}^{n}$, where $0 < s < e < n$. We generate $\hat{\mathcal{M}}$ connecting endpoints $\boldsymbol{p}_{s-1}^N$ and $\boldsymbol{p}_{r+1}^C$ via a learnable function f_θ, given $\mathcal{U}$ with a fixed conformation as input:

$$\hat{\mathcal{M}} = f_\theta(\boldsymbol{p}|\mathcal{U}, x), x \sim \mathcal{N}(0, \mathbf{I}) \tag{1}$$

Note that θ indicates learnable parameters, x is a set of structural variables, such as coordinates and folding angles introduced later. The designed $\hat{\mathcal{M}}$ should be non-trivial to satisfy the following constraints:

1. Protein likeness: The designed structures are likely to constitute natural proteins.
2. Connectivity: $\hat{\mathcal{M}}$ should effectively connect $\boldsymbol{p}_{s-1}^N$ and $\boldsymbol{p}_{e+1}^C$ without breakage.
3. Non-overlapping: The designed structure $\hat{\mathcal{M}}$ should not overlap with existing structure $\mathcal{U}$.

3D Molecule Generation. Generating 3D molecules to explore the local minima of the energy function (Conformation Generation) (Gebauer et al., 2019; Simm et al., 2020b;a; Shi et al., 2021; Xu et al., 2021; Luo et al., 2021; Xu et al., 2020; Ganea et al., 2021; Xu et al., 2022; Hoogeboom et al., 2022; Jing et al., 2022; Zhu et al., 2022) or discover potential drug molecules binding to targeted proteins (3D Drug Design) (Imrie et al., 2020; Nesterov et al., 2020; Luo et al., 2022; Ragoza et al., 2022; Wu et al., 2022b; Huang et al., 2022a; Peng et al., 2022; Huang et al., 2022b; Wang et al., 2022b; Liu et al., 2022b) have attracted extensive attention in recent years. Compared to conformation generation that aims to predict the set of favorable conformers from the molecular graph, 3D Drug Design is more challenging in two aspects: (1) both conformation and molecule graph need to be generated, and (2) the generated molecules should satisfy multiple constraints, such as physical prior and protein-ligand binding affinity. We summarized representative works of 3D drug design in Table.5 in the appendix, where all the methods focus on small molecule design.

Protein Design. In addition to small molecules, biomolecules such as proteins have also attracted considerable attention from researchers (Ding et al., 2022; Ovchinnikov & Huang, 2021; Gao et al., 2020; Strokach & Kim, 2022). We divide the mainstream protein design methods into three categories: protein sequence design (Li et al., 2014; Wu et al., 2021; Pearce & Zhang, 2021; Ingraham et al., 2019;

Jing et al., 2020; Tan et al., 2022; Gao et al., 2022a; Hsu et al., 2022; Dauparas et al., 2022; Gao et al., 2022b; O'Connell et al., 2018; Wang et al., 2018; Qi & Zhang, 2020; Strokach et al., 2020; Chen et al., 2019; Zhang et al., 2020; Anand & Achim, 2022), unconditional protein structure generation (Anand & Huang, 2018; Sabban & Markovsky, 2020; Eguchi et al., 2022; Wu et al., 2022a), and conditional protein design (Lee & Kim, 2022; Wang et al., 2022a; Trippe et al., 2022; Lai et al., 2022; Fu & Sun, 2022; Tischer et al., 2020; Anand & Achim, 2022; Luo et al.). Protein sequence design aims to discover protein sequences folding into the desired structure, and unconditional protein structure generation focuses on generating new protein structures from noisy inputs. We are interested in conditional protein design and consider multiple constraints on the designed protein. For example, Wang's model (Wang et al., 2022a), SMCDiff (Trippe et al., 2022) and Tischer's model (Tischer et al., 2020) design the scaffold for the specified functional sites. ProteinSGM (Lee & Kim, 2022) mask short spans (< 8 residues) of different secondary structures in different structures and treats the design task as an inpainting problem. CoordVAE (Lai et al., 2022) produces novel protein structures conditioned on the backbone template. RefineGNN (Jin et al., 2021), CEM (Fu & Sun, 2022), and DiffAb (Luo et al.) aim to generate the complementarity-determining regions of the antibody. We summarized the protein design model in Table.6.

Sequence Diffusion for Protein Structure Generation. Diffusion models (Sohl-Dickstein et al., 2015; Ho et al., 2020; Cao et al., 2022) are a class of generative models that have achieved impressive results in image (Song et al., 2020; Lugmayr et al., 2022; Whang et al., 2022; Baranchuk et al., 2021; Wolleb et al., 2022), speech (Lee & Han, 2021; Chen et al., 2020; Kong et al., 2020; Liu et al., 2022a) and text (Li et al., 2022; Chen et al., 2022; Austin et al., 2021) synthesis. Recently, FoldingDiff (Wu et al., 2022a) shows that sequence models could be used for unconditional protein generation.

2 Background and Knowledge Gap

Considering three backbone atoms (N, C_α, C) for each residue, there are 9 $(= 3 \times 3)$ freedom degrees are required for 3D representation. Recently, researchers have introduced human knowledge into protein backbone representation and proposed two simplified approaches: frame-based and angle-based representation, as shown in Fig.2 (a).

Frame-based. This approach (Jumper et al., 2021) treats residues as fundamental elements and assumes that residues of the same type have the same rigid structure, called the local frame. As shown in Fig.2 (a), we write $F_i = \{C_i, C_{\alpha_i}, N_i\}$ as the local frame of the i-th residue, where position $\boldsymbol{p}_{F_i}$, orientation R_i and the residue type s_i are required for describing F_i, resulting in 7$(= 3 + 3 + 1)$ freedom degrees. Under this representation, geometric features can be computed efficiently, e.g., pairwise distance and relative positions. However, the model needs to consider the geometric equivariance of the input data, which introduces considerable modeling complexity.

Angle-based. This approach converts structures into sequences of backbone angles based on the order of the protein's primary structure; see Fig.2 (a). By assuming the backbone bond lengths are fixed, three bond angles $\alpha_i^N, \alpha_i^A, \alpha_i^C$ and three torsion angles $\beta_i^N, \beta_i^A, \beta_i^C$ are required for describing one residue, leading to 6 freedom degrees. The reduced freedom forms a more compact representation than the frame-based approach. In addition, there is no need to consider geometric equivariance since all angles are invariant to spatial rotation and translation.

Geometric Constraints. The angle-based representation seems attractive for simplifying structural modeling and learning more compact protein representations. However, it suffers from the drawback of inefficient computing of geometric features, making it challenging to consider geometric constraints. For example, if one wants to optimize

$$\mathcal{L}_{dist} = \min_{\{\alpha_i^N,\alpha_i^A,\alpha_i^C,\beta_i^N,\beta_i^A,\beta_i^C\}_0^i} (||\boldsymbol{p}_i^A - \boldsymbol{p}_1^A|| - r)^2 \tag{2}$$

given $\boldsymbol{p}_1^N, \boldsymbol{p}_1^A, \boldsymbol{p}_1^C$. Then, $\boldsymbol{p}_2^N \rightarrow \boldsymbol{p}_2^A \rightarrow \boldsymbol{p}_2^C \rightarrow \boldsymbol{p}_3^N \rightarrow \boldsymbol{p}_3^A \rightarrow \cdots \rightarrow \boldsymbol{p}_i^A$ needs to be recursively computed by

$$\begin{cases} \boldsymbol{p}_i^N = \text{Place}(\boldsymbol{p}_{i-1}^C, \alpha_{i-1}^N, \beta_{i-1}^N, \boldsymbol{d}_{i-1}^C, \boldsymbol{d}_{i-1}^A, r^N) \\ \boldsymbol{p}_i^A = \text{Place}(\boldsymbol{p}_i^N, \alpha_i^A, \beta_{i-1}^A, \boldsymbol{d}_i^N, \boldsymbol{d}_{i-1}^C, r^A) \\ \boldsymbol{p}_i^C = \text{Place}(\boldsymbol{p}_i^A, \alpha_i^C, \beta_i^C, \boldsymbol{d}_i^A, \boldsymbol{d}_i^N, r^C) \end{cases} \tag{3}$$

where $\boldsymbol{d}_i^N = \frac{\boldsymbol{p}_i^N - \boldsymbol{p}_{i-1}^C}{||\boldsymbol{p}_i^N - \boldsymbol{p}_{i-1}^C||}, \boldsymbol{d}_i^A = \frac{\boldsymbol{p}_i^A - \boldsymbol{p}_i^N}{||\boldsymbol{p}_i^A - \boldsymbol{p}_i^N||}, \boldsymbol{d}_i^C = \frac{\boldsymbol{p}_i^C - \boldsymbol{p}_i^A}{||\boldsymbol{p}_i^C - \boldsymbol{p}_i^A||}$. Note that backbone bond lengths, e.g., $r^N = ||\boldsymbol{p}_i^N - \boldsymbol{p}_{i-1}^C||, r^A = ||\boldsymbol{p}_i^A - \boldsymbol{p}_i^N||, r^C = ||\boldsymbol{p}_i^C - \boldsymbol{p}_i^A||$, are constants. Alg.1 (in the appendix) shows the details of place$(\boldsymbol{p}, \alpha, \beta, \boldsymbol{d}_1, \boldsymbol{d}_2)$.

GradCurse. The aforementioned symbols N, A, and C are used to identify the backbone atoms. To simplify notation, let's rewrite $\{\boldsymbol{p}_1^A, \boldsymbol{p}_1^C, \boldsymbol{p}_2^N, \boldsymbol{p}_2^A, \boldsymbol{p}_2^C, \cdots, \boldsymbol{p}_i^N, \boldsymbol{p}_i^A\}$ as $\{\boldsymbol{x}_0, \boldsymbol{x}_1, \boldsymbol{x}_2, \boldsymbol{x}_3, \cdots, \boldsymbol{x}_{n-1}, \boldsymbol{x}_n\}$. We define $\boldsymbol{d}_i = \frac{\boldsymbol{x}_i - \boldsymbol{x}_{i-1}}{||\boldsymbol{x}_i - \boldsymbol{x}_{i-1}||}$, $r_i = ||\boldsymbol{x}_i - \boldsymbol{x}_{i-1}||$, $\boldsymbol{e} = \frac{\boldsymbol{x}_n - \boldsymbol{x}_0}{||\boldsymbol{x}_n - \boldsymbol{x}_0||}$, and $L = \sum_{i=1}^n r_i \boldsymbol{e}^T \boldsymbol{d}_i$. Consequently, Equation 2 can be reformulated as $\mathcal{L}(\sum_{i=1}^n r_i \boldsymbol{e}^T \boldsymbol{d}_i; r)$. As proved in the appendix, under mild assumptions, the projected gradient along the $\boldsymbol{e}$ direction is:

$$\frac{\partial \mathcal{L}}{\partial \boldsymbol{d}_i} \boldsymbol{e} = \frac{\partial \mathcal{L}}{\partial L} (\sum_{k=i}^{n} r_k \boldsymbol{e}^T \frac{\partial \boldsymbol{d}_k}{\partial \boldsymbol{d}_i} \boldsymbol{e}) \tag{4}$$

where the expected value of $\boldsymbol{e}^T \frac{\partial \boldsymbol{d}_n}{\partial \boldsymbol{d}_{n-k}} \boldsymbol{e}$ could be estimated as:

$$\mathbb{E}[\boldsymbol{e}^T \frac{\partial \boldsymbol{d}_n}{\partial \boldsymbol{d}_{n-k}} \boldsymbol{e}] \approx K_1 t_1^k + K_2 t_2^k \tag{5}$$

Here, K_1, K_2, t_1, t_2 are constants. The Eq.5 shows that the projected gradient is either exploding or vanishing, resulting in unstable training. We observe this phenomenon in our experiments and call this phenomenon **GradCurse** of angle-based representation methods.

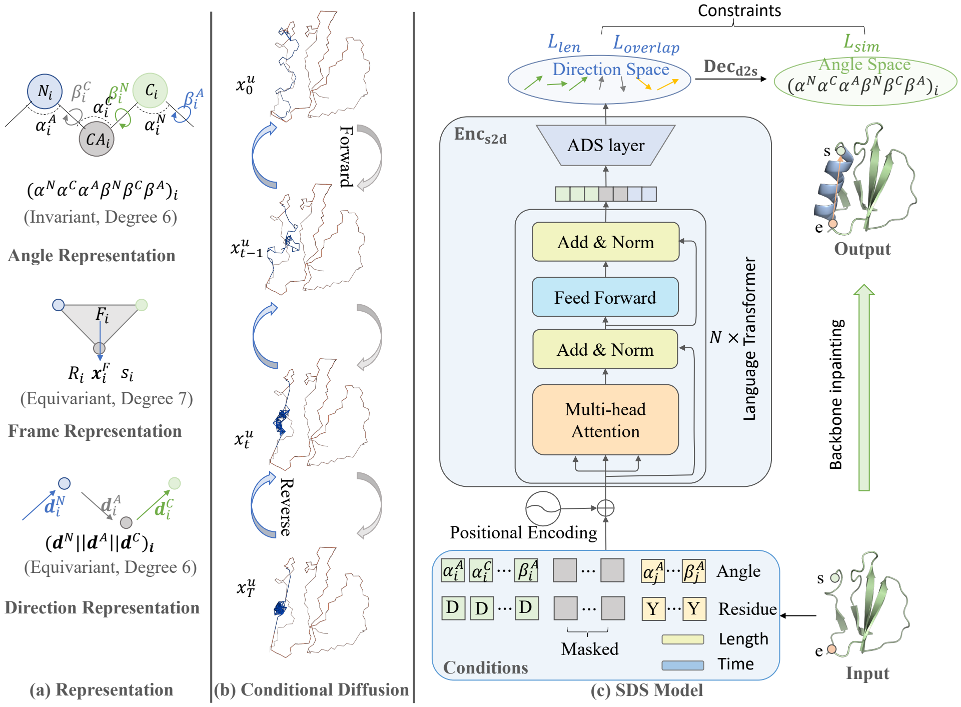

Figure 2: The overall framework. (a) We introduce a new direction representation for efficiently computing geometric features while enjoying minimal freedom. (b) Only the masked structures are involved in the diffusion process, while the unmasked ones remain fixed. (c) We add an ADS layer upon the sequence transformer to convert invariant features into equivariant directions, namely Enc_{s2d}. Then the Dec_{d2s} reverses directions as invariant features based on Eq.17. The geometric constraints ($\mathcal{L}_{len}$ and $\mathcal{L}_{overlap}$) could be efficiently imposed on the direction space. The overall $\text{Enc}_{\text{s2d}} + \text{Dec}_{\text{d2s}}$ is a simple sequence model. Remind that the term ”mask” may be abused here as we corrupt the angles with wrapped Gaussian noise instead of replacing them with a special mask token.

3 METHOD

3.1 OVERALL FRAMEWORK & NOVEL REPRESENTATION

We introduce a novel direction-based representation for protein backbone, which enjoys the simplicity of angle-based representations while effectively mitigating the issue of GradCurse. Based on the direction-based representation, we propose a sequence diffusion model for constrained protein backbone inpainting, called DiffSDS. The model takes unmasked atoms and controllable conditions as input to recover the masked region, as shown in Fig.2.

Direction-based Representation. Is there an alternative representation beyond frame- and angle-based ones to support efficient computation of geometric features while enjoying low degrees of freedom? As shown in Fig.2(a), we introduce direction vectors, i.e., $\boldsymbol{d}_i^A, \boldsymbol{d}_i^N, \boldsymbol{d}_i^C$, for discribing protein structures. In the direction-based representation, the position of each atom is determined by its relative direction ($\boldsymbol{d}_i^A, \boldsymbol{d}_i^N, \boldsymbol{d}_i^C$) and distance ($r^N, r^A, r^C$) from its parent node. In Fig.2(a), taking C_α as an example,

$$\boldsymbol{p}_i^A = \boldsymbol{p}_i^N + r^A \boldsymbol{d}_i^A \tag{6}$$

Recall that $\boldsymbol{p}_i^A$ and $\boldsymbol{p}_i^N$ are spatial coordinates of C_{α_i} and N_i. The direction vector $\boldsymbol{d}_i^A$ points from $\boldsymbol{p}_i^N$ to $\boldsymbol{p}_i^A$, and r^A is the length of the $C_\alpha - C$ bond.

Advantages. The proposed representation has several advantages. Firstly, the computing cost of relative positions will be reduced. For example, when computing $\boldsymbol{p}_i^A - \boldsymbol{p}_0^A$, only parallel linear additions and multiplications are required, without recursive computation as in Eq.3:

$$\boldsymbol{p}_i^A - \boldsymbol{p}_0^A = r^A \sum_{k=2}^{i} \boldsymbol{d}_i^A + r^C \sum_{k=1}^{i-1} \boldsymbol{d}_i^C + r^N \sum_{k=2}^{i} \boldsymbol{d}_i^N \tag{7}$$

Secondly, there is no gradient vanishing or exploding issue in Eq.7. Thirdly, this representation enjoys the lowest 6 freedom degrees since $||\boldsymbol{d}_i^A|| = ||\boldsymbol{d}_i^C|| = ||\boldsymbol{d}_i^N|| = 1$. Finally, direction representation could be equivalently transformed to the angle-based one, as shown in Eq.17 in the appendix.

3.2 DUAL-SPACE DIFFUSION MODEL

We propose a sequence diffusion model f_θ equipped with direction space for recovering masked backbone $\mathcal{M}$ conditional on the unmasked part $\mathcal{U}$:

$$\hat{\mathcal{M}} = f_\theta(\boldsymbol{p}|\mathcal{U}, x), x \sim \mathcal{N}(0, \mathbf{I}) \tag{8}$$

f_θ consists multiple bert transformer layers, to which we add an ADS layer, i.e., a linear projection head $\text{ADS}(\boldsymbol{h}) : \boldsymbol{h} \in \mathbb{R}^{n,d_h} \rightarrow \boldsymbol{d} \in \mathbb{R}^{n,3}$, to convert hidden feature vectors $\boldsymbol{h}$ as direction vectors $\boldsymbol{d}$.

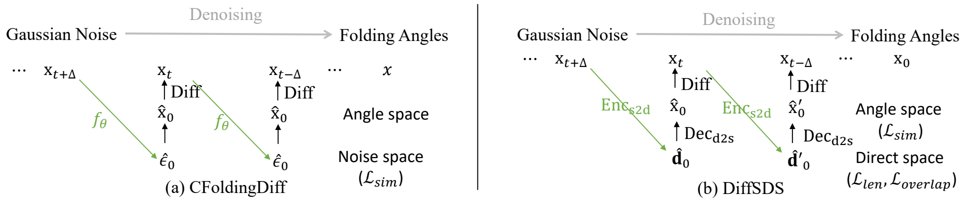

Figure 3: Reverse diffusion. (a) FoldingDiff uses the neural model f_θ to predict one-step noise, where angular similarity loss is imposed on the noise space. We extend FoldingDiff to conditional scenes by fixing the unmasked structure during diffusion to obtain CFoldingDiff. (b) DiffSDS uses Enc$_{\text{s2d}}$ to predict the direction representation of the original protein. The angular similarity loss and geometric constraints are imposed in the angle and direction space, respectively.

Conditions. The model takes multiple prior conditions as input features for each residue, as shown in Fig.2(c). The node-level conditional features include backbone angles $F_{ang} \in \mathbb{R}^{n,6}$, and residue type embedding $F_{res} \in \mathbb{R}^{n,20}$ of unmasked residues. The global-level conditional features include the length ($F_{len} \in \mathbb{R}$) of the masked fragment and diffusion timestamp ($F_{time} \in \mathbb{R}$).

Conditional Forward Diffusion. The forward diffusion process could be viewed as a mixup path from clean data $x_0 \sim p_{data}$ to noise $x_T \sim \mathcal{N}(0, I)$: $x_0 \to x_1 \to \cdots \to x_T$. Different from generating proteins from scratch, the structure $\mathcal{U}$ is given as a prior, whose angles should not be changed during the diffusion process. Therefore, we divide the latent variable x_t into two parts: $x_t = x_t^m \bigoplus x_t^u$, where x_t^m and x_t^u are the masked and unmasked protein angles at timestamp t. Denote $\alpha_0 = 1, \sigma_0 = 0, q(x_0|x_0) = \mathcal{N}(x_0; \alpha_0 x, \sigma_0^2 I)$, we have

$$q(x_t^m|x_0^m) = \mathcal{N}_{\text{wrapped}}(x_t^m; \alpha_t x_0^m, \sigma_t^2 I) \propto \sum_{k=-\infty}^{\infty} \exp\left(\frac{-||x_t^m - \alpha_t x_0^m + 2\pi k||}{2\sigma_t^2}\right) \tag{9}$$

where we use the wrapped normal (Wu et al., 2022a) to force the angles space in $[0, \pi]$. The hyper-parameters α_t and σ_t determine the diffusion schedule, i.e., $\sigma_t = \text{clip}(1 - \alpha_t, 0.999)$ and $\alpha_t = \cos\left(t/T \cdot \frac{\pi}{2}\right)$.

Direction-aware Reverse Diffusion. The reverse process applies neural network f_θ as the translation kernel to recover clean data following the Markov chain $x_T \to x_{T-1} \to \cdots \to x_0$. As derived in the Appendix, the objective is to maximize $q(x_{t-1}|x_t, x_0) = \mathcal{N}(z_{t-1}; \hat{\mu}_{t-1}, \hat{\sigma}_{t-1}^2 I)$, and

$$\begin{cases} \hat{\sigma}_s = \frac{\sigma_{t|s}\sigma_s}{\sigma_t} \\ \hat{\mu}_s = \frac{1}{\alpha_{t|s}} x_t - \frac{\alpha_{t|s}}{\sigma_t} \epsilon_t \end{cases} \tag{10}$$

There are several alternative variables could be estimated by f_θ to obtain $q(x_{t-1}|x_t, x_0)$, such as $\hat{\mu}_{t-1}, \hat{\epsilon}_{t-1}, \hat{x}_0$. As shown in Fig.3, FoldingDiff realizes the neural network as $f_\theta : (x_t, t) \mapsto \hat{\epsilon}_t$, which is effective for unconditional protein backbone generation. Instead, we prefer $f_\theta : (x_t, t) \mapsto \hat{x}_0$ and decompose it as encoder Enc_{s2d} and decoder Dec_{d2s}. The $\text{Enc}_{\text{s2d}} : (x_t, t) \mapsto \hat{d}_0$ predicts the direction vectors (d_0) of the backbone, and the decoder $\text{Dec}_{\text{d2s}} : \hat{d}_0 \mapsto \hat{x}_0$ reverses the direction representation into angle representation based on Eq.17. With the inserted direction space, we could efficiently compute geometric features from and impose corresponding constraints on the model, as illustrated in Eq.6 and Eq.2. More importantly, this modification does not increase the modeling complexity: f_θ still appears as a sequence model, with the inputs and outputs being sequences.

3.3 Constraints

Protein Likeness. From the diffusion perspective, the neural model needs to recover the masked backbone angles to ensure the protein likeness. The overall objective is to maximize the variational lower bound of $\log p_\theta(x_0)$:

$$\mathcal{L}_{vlb}(x_0) = \mathop{\mathbb{E}}_{q(x_{1:T}|x_0)} \left[\log \frac{q(x_T|x_0)}{p_\theta(x_T)} + \sum_{t=2}^{T} \log \frac{q(x_{t-1}|x_0, x_t)}{p_\theta(x_{t-1}|x_t)} - \log p_\theta(x_0|x_1) \right] \tag{11}$$

In practice, we use the simplfied loss: $\mathcal{L}_{sim}(x_0) = \sum_{t=0}^{T} ||f_\theta(x_t, t) - x_0||^2$.

Length Loss. To ensure the designed $\hat{\mathcal{M}}$ has a similar length as the reference structure $\mathcal{M}$, such that the masked endpoints (s and e) could be connected, we employ the following loss on the direction space:

$$\mathcal{L}_{len} = \sum_{S \in \{N, A, C\}} (||\hat{\boldsymbol{p}}_s^S - \hat{\boldsymbol{p}}_e^S|| - ||\boldsymbol{p}_s^S - \boldsymbol{p}_e^S||)^2 \tag{12}$$

where $\hat{\boldsymbol{p}}_s^S - \hat{\boldsymbol{p}}_e^S$ are computed by Eq.7 using the output directions of Enc_{s2d}.

Overlapping Loss. To avoid overlapping between designed $\hat{\mathcal{M}}$ and unmasked structure $\mathcal{U}$, the overlapping loss is also imposed on the direction space:

$$\mathcal{L}_{overlap} = \sum_{i \in [s+1, e-1]} e^{-\tau ||\hat{\boldsymbol{p}}_i^A - \boldsymbol{p}_j^A||} \tag{13}$$

where $j = \min_{j \in [1,s] \cup [e,n]} ||\boldsymbol{p}_i^A - \boldsymbol{p}_j^A||$ is the nearst α-carbon atom to $\hat{\boldsymbol{p}}_i^A$ in $\mathcal{U}$. We set $\tau = 0.8$.

Overall Loss. During training, we impose protein similarity loss ($\mathcal{L}_{sim}$), length loss ($\mathcal{L}_{len}$), and overlapping loss ($\mathcal{L}_{overlap}$) on the model, the overall loss function is:

$$\mathcal{L} = \lambda_1 \mathcal{L}_{sim} + \lambda_2 \mathcal{L}_{len} + \lambda_3 \mathcal{L}_{overlap} \tag{14}$$

where we choose $\lambda_1 = 1, \lambda_2 = 0.001, \lambda_3 = 10$.

4 Experiments

In this section, we conduct experiments to answer the following questions:

- **Q1: Comparision.** Could DiffSDS outperform the angle-based CFoldingDiff and even demonstrate competitive results comparable to frame-based models?
- **Q2: Ablation.** Does the conditional features and constraints improves performance?

4.1 Overall Setting

Data Split. We train models on CATH4.3, where proteins are partitioned by the CATH topology classification. To avoid potential information leakage, we further refine the test set by excluding proteins that are similar to the training data from the test set, i.e., TM-score greater than 0.5. Finally, there are 24,199 proteins for training, 3,094 proteins for validation, and 378 proteins for testing.

Baselines. We compare DiffSDS with recent sequence modeling baselines (CFoldingDiff) and coordinates diffusion baselines (SMCDiff (Trippe et al., 2022), RFDesign (Wang et al., 2022a), and RFDiffusion (Watson et al., 2023)). CFoldingDiff is a derivative of FoldingDiff (Wu et al., 2022a) where the angles and residue types of the unmasked residues are fixed during diffusion. RFDesign and RFDiffusion are state-of-the-art structural models trained across the whole PDB dataset and accepted by Science and Nature, respectively. While there are other interesting protein structure generative models, such as IG-VAE (Eguchi et al., 2022), Genie (Lin & AlQuraishi, 2023), and FrameDiff (Yim et al., 2023), it is important to note that they focus on unconditional generation instead of conditional inpainting.

Setting. We evaluate all methods on the same test dataset, where the contiguous backbones of length $m \sim U(5, L/3)$ are randomly masked, given the protein length L. For the same protein, the masked area remains the same when evaluating different methods. We retrain CFoldingDiff to make it suitable for the inpainting task, while the pre-trained SMCDiff, RFDesign and RFDiffusion can be used directly. For DiffSDS, we utilize 16 transformer layers with 384 hidden dimensions and 12 attention heads per layer. CFoldingDiff and DiffSDS are trained for up to 10,000 epochs with an early stopping patience of 1,000. The learning rate is set to 0.0001, the batch size to 128, and the maximum diffusion timestamp T to 1,000.

4.2 Protein Likeness

Objective & Setting. Are the designed structures likely to constitute native proteins? We take Rosetta energies (rama and omega) as metrics to measure the protein likeness of the generated backbones. The ”rama” indicates Ramachandran torsion energy derived from statistics on the PDB, and ”omega” indicates omega angle energy. In the appendix, we show the angle distributions and Ramachandran plots of the different methods in Fig.6. We group results by the masked length to reveal the performance at different mask lengths. We also adopt the energy of the test set structures as a baseline to show how closely we approximate the reference structures.

Representation	energy	rama (↓)			omega (↓)		
	mask length	<15	15-30	>30	<15	15-30	>30
	Test	0.67	0.71	0.62	0.75	0.68	0.66
Frame-based	RFDesign	2.12	2.49	3.38	16.62	12.56	13.14
	RFDiffusion	**1.19**	**1.11**	**0.87**	**1.36**	**1.2**	**1.21**
Angle-based	CFoldingDiff	1.65	1.86	2.11	6.26	4.97	4.17
	DiffSDS	**1.51**	**1.76**	**1.95**	**4.30**	**3.17**	**2.77**

Table 1: Rosetta energies of generated backbones. We highlight the **best** results within each group.

Results & Analysis. We present results in Table.1. DiffSDS outperforms angle-based CFoldingDiff and provides competitive results compared to frame-based methods. The improvements to CFoldingDiff are consistent in terms of different masked lengths. However, we also observe that there still exists a considerable performance gap between the angle-based methods and the best frame-based RFDiffusion, where DiffSDS is the first attempt to fill this gap. In Figure.6, we compare the angular distributions of different methods, where DiffSDS's results are close to the test set distribution.

4.3 Connectivity

Objective & Setting. Do the designed structures connect the endpoints without breakage? As shown in Figure.1, the connectivity is an important indicator for the inpainting task, as disconnected proteins must be structurally abnormal. However, this metric has lacked attention in previous work, and we begin by defining the connectivity error as:

$$\text{Error} = ||\boldsymbol{p}_s^A - \hat{\boldsymbol{p}}_s^A|| + ||\boldsymbol{p}_e^A - \hat{\boldsymbol{p}}_e^A|| \tag{15}$$

where s and e are indexes of the start and end points of the masked structure, $\hat{\boldsymbol{p}}^A$ and $\boldsymbol{p}^A$ indicate the predicted and ground truth positions of the C_α-carbon. Ideally, Error $= 0$ means that endpoints are connected as expected.

Results & Analysis. From Table.2, we conclude that DiffSDS could achieve the lowest connectivity error compared to baselines. We identify that good connectiveness is a significant difference made by DiffSDS, as explicitly imposing geometric constraints on the direction space could avoid structural breaks. Despite the protein-like appearance of the generated fragment, previous frame-based methods fail to ensure connectiveness, resulting in an overall flawed inpainted protein structure. We further show the trend of connectivity error with increasing mask length in Figure.7, from which we find that SMCDiff and RFDesign perform poorly at all mask lengths, FoldingDiff's connectivity error increases with mask length, while DiffSDS performs steadily and consistently better than all baselines.

Representation		Connectivity error (↓)		
	mask length	<10	10-15	>15
Frame-based	SMCDiff	**113.62**	**107.32**	**154.52**
	RFDesign	218.36	146.24	159.17
	RFDiffusion	213.21	141.99	158.67
Angle-based	CFoldingDiff	14.77	42.65	59.08
	DiffSDS	**6.93**	**9.93**	**10.61**

Table 2: Connectivity error of different methods.

4.4 Non-overlapping

Objective & Setting. Will the designed structures be overlapped with existing backbones? We evaluate the spatial interaction between the generated structure ($\hat{\mathcal{M}}$) and the unmasked structure ($\mathcal{U}$), and define the interaction score as

$$\text{Score}_d = \sum_{i \in \hat{\mathcal{M}}, j \in \mathcal{U}} \mathbb{1}(||\hat{\boldsymbol{x}}_i - \hat{\boldsymbol{x}}_j|| < d) \tag{16}$$

where $\mathbb{1}(\cdot)$ is an indicator function. Score$_d$ records the number of pairwise interactions between masked and non-masked amino acids, with distances threshold d $\mathring{A}$.

Representation		$d = 1\mathring{A}$			$d = 3\mathring{A}$		
	mask length	<15	15-30	>30	<15	15-30	>30
	True	266	345	139	268	406	139
Frame-based	RFDesign	280	357	153	861	1362	593
	RFDiffusion	**266**	**345**	**139**	**275**	**347**	**139**
Angle-based	CFoldingDiff	276	**352**	145	552	640	222
	DiffSDS	**270**	356	**141**	**472**	**632**	**178**

Table 3: The number of spatial interactions.

Results & Analysis. As shown in Table.3, the spatial interactions of DiffSDS's generated structures are closer to the test set than the CFoldingDiff. This verifies that incorporating a non-overlap loss in the direction space can be beneficial for angle-based methods in generating reasonable structures.

4.5 Ablation Study

Objective&Setting. We conduct ablation experiments to investigate the impact of conditions and constraints on protein backbone inpainting. Specifically, we show how these factors affect the validation losses, including angle loss, length loss, and overlapping loss.

Results & Analysis. Limited to the page, we show the ablation details in the Appendix. As shown in Fig.8 and Fig.9, we find that: (1) the length condition and the sequence condition contribute to the reduction of $\mathcal{L}_{len}$ and $\mathcal{L}_{sim}$, respectively. This phenomenon suggests that the model can learn to generate structures with a predetermined length and that residue types can facilitate learning backbone angles. (2) Explicitly imposing geometric constraints on the model is necessary. If the constraints are removed, the $\mathcal{L}_{len}$ loss is difficult to reduce, and the $\mathcal{L}_{overlap}$ even increases, indicating the model could not generate geometrically reasonable structures. Fortunately, all these drawbacks could be eliminated by imposing geometric loss on the introduced direction space.

4.6 Designability

Objective & Setting. How likely are the generated proteins to be synthesized in the laboratory? We further measure the designability of the generated protein by the self-consistency TM score (scTM), which is first introduced by FoldingDiff. The generated backbones are fed into ESM-IF to obtain candidate protein sequences, which are subsequently folded into 3D structures by OmegaFold. scTM is the TM score between the newly folded structure and the original generated structure. If scTM> 0.5, the corresponding generated backbone is considered designable.

Results & Analysis. As shown in Table4, the designability order is: RFDiffusion > DiffSDS>CFoldingDiff>RFDesign>SMCDiff. On the full test set, DiffSDS generates 231 designable backbones, outperforming CFoldingDiff's 217 and RFDesign's 178. Compared with CFoldingDiff, DiffSDS achieves consistent improvements in all settings. The pure transformer-based DiffSDS, without considering the equivariance, even outperforms several frame-based methods, such as SMCDiff and RFDesign. Despite the gap from RFDiffusion is still large, DiffSDS presents a new modeling paradigm and promising results for protein structure generation. In Fig.4, we show a protein inpainting example, comparing different methods. Combine with Table.2, we argue that structural breaks due to the lack of structural constraints would corrupt the input features of ESM-IF for SMCDiff and RFDesign, producing poor sequence design and ultimately poor scTM scores.

Representation		scTM>0.5 (↑)			scTM (↑)	
		All	len≤70	len>70	Mean	Median
Frame-based	SMCDiff	30/378	12/148	18/230	0.36	0.34
	RFDesign	178/378	65/148	113/230	0.51	0.48
	RFDiffusion	**255/378**	**103/148**	**152/230**	**0.60**	**0.59**
Angle-based	CFoldingDiff	217/378	81/148	130/230	0.54	0.53
	DiffSDS	**231/378**	**88/148**	**143/230**	**0.56**	**0.55**

Table 4: Designability of different methods.

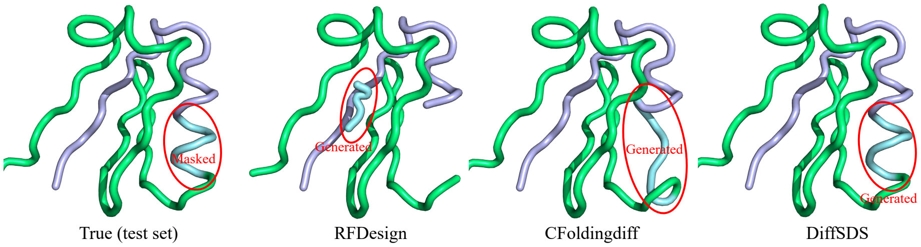

True (test set) RFDesign CFoldingdiff DiffSDS

Figure 4: Inpating examples. DiffSDS generates a more similar structure to the reference protein.

5 Conclusion

This paper enhances the pure-transformer as a strong structure learner by introducing a hidden direction-based space. The proposed method not only maintains the simplicity of sequence modeling but also enables efficient and effective computation of geometric features, avoiding the issue of GradCurse. By employing the model within the framework of conditional diffusion, the proposed DiffSDS bridges the gap between angle-based and frame-based diffusion models, surpassing the angle-based CFoldingDiff method, and introducing a new paradigm for protein structure learning.

References

Namrata Anand and Tudor Achim. Protein structure and sequence generation with equivariant denoising diffusion probabilistic models. *arXiv preprint arXiv:2205.15019*, 2022.

Namrata Anand and Possu Huang. Generative modeling for protein structures. *Advances in neural information processing systems*, 31, 2018.

Jacob Austin, Daniel D Johnson, Jonathan Ho, Daniel Tarlow, and Rianne van den Berg. Structured denoising diffusion models in discrete state-spaces. *Advances in Neural Information Processing Systems*, 34:17981–17993, 2021.

Dmitry Baranchuk, Ivan Rubachev, Andrey Voynov, Valentin Khrulkov, and Artem Babenko. Label-efficient semantic segmentation with diffusion models. *arXiv preprint arXiv:2112.03126*, 2021.

Hanqun Cao, Cheng Tan, Zhangyang Gao, Guangyong Chen, Pheng-Ann Heng, and Stan Z Li. A survey on generative diffusion model. *arXiv preprint arXiv:2209.02646*, 2022.

Nanxin Chen, Yu Zhang, Heiga Zen, Ron J Weiss, Mohammad Norouzi, and William Chan. Wavegrad: Estimating gradients for waveform generation. *arXiv preprint arXiv:2009.00713*, 2020.

Sheng Chen, Zhe Sun, Lihua Lin, Zifeng Liu, Xun Liu, Yutian Chong, Yutong Lu, Huiying Zhao, and Yuedong Yang. To improve protein sequence profile prediction through image captioning on pairwise residue distance map. *Journal of chemical information and modeling*, 60(1):391–399, 2019.

Ting Chen, Ruixiang Zhang, and Geoffrey Hinton. Analog bits: Generating discrete data using diffusion models with self-conditioning. *arXiv preprint arXiv:2208.04202*, 2022.

Justas Dauparas, Ivan Anishchenko, Nathaniel Bennett, Hua Bai, Robert J Ragotte, Lukas F Milles, Basile IM Wicky, Alexis Courbet, Rob J de Haas, Neville Bethel, et al. Robust deep learning based protein sequence design using proteinmpnn. *bioRxiv*, 2022.

Wenze Ding, Kenta Nakai, and Haipeng Gong. Protein design via deep learning. *Briefings in bioinformatics*, 23(3):bbac102, 2022.

Justin A Drake and B Montgomery Pettitt. Physical chemistry of the protein backbone: Enabling the mechanisms of intrinsic protein disorder. *The Journal of Physical Chemistry B*, 124(22): 4379–4390, 2020.

Raphael R Eguchi, Christian A Choe, and Po-Ssu Huang. Ig-vae: Generative modeling of protein structure by direct 3d coordinate generation. *Biorxiv*, pp. 2020–08, 2022.

Noelia Ferruz, Michael Heinzinger, Mehmet Akdel, Alexander Goncearenco, Luca Naef, and Christian Dallago. From sequence to function through structure: deep learning for protein design. *Computational and Structural Biotechnology Journal*, 2022.

Tianfan Fu and Jimeng Sun. Antibody complementarity determining regions (cdrs) design using constrained energy model. In *Proceedings of the 28th ACM SIGKDD Conference on Knowledge Discovery and Data Mining*, pp. 389–399, 2022.

Octavian Ganea, Lagnajit Pattanaik, Connor Coley, Regina Barzilay, Klavs Jensen, William Green, and Tommi Jaakkola. Geomol: Torsional geometric generation of molecular 3d conformer ensembles. *Advances in Neural Information Processing Systems*, 34:13757–13769, 2021.

Wenhao Gao, Sai Pooja Mahajan, Jeremias Sulam, and Jeffrey J Gray. Deep learning in protein structural modeling and design. *Patterns*, 1(9):100142, 2020.

Zhangyang Gao, Cheng Tan, Stan Li, et al. Alphadesign: A graph protein design method and benchmark on alphafolddb. *arXiv preprint arXiv:2202.01079*, 2022a.

Zhangyang Gao, Cheng Tan, and Stan Z Li. Pifold: Toward effective and efficient protein inverse folding. *arXiv preprint arXiv:2209.12643*, 2022b.

Niklas Gebauer, Michael Gastegger, and Kristof Schütt. Symmetry-adapted generation of 3d point sets for the targeted discovery of molecules. *Advances in neural information processing systems*, 32, 2019.

Niklas WA Gebauer, Michael Gastegger, Stefaan SP Hessmann, Klaus-Robert Müller, and Kristof T Schütt. Inverse design of 3d molecular structures with conditional generative neural networks. *Nature communications*, 13(1):1–11, 2022.

Jonathan Ho, Ajay Jain, and Pieter Abbeel. Denoising diffusion probabilistic models. *Advances in Neural Information Processing Systems*, 33:6840–6851, 2020.

Emiel Hoogeboom, Vıctor Garcia Satorras, Clément Vignac, and Max Welling. Equivariant diffusion for molecule generation in 3d. In *International Conference on Machine Learning*, pp. 8867–8887. PMLR, 2022.

Chloe Hsu, Robert Verkuil, Jason Liu, Zeming Lin, Brian Hie, Tom Sercu, Adam Lerer, and Alexander Rives. Learning inverse folding from millions of predicted structures. *bioRxiv*, 2022.

Lei Huang, Hengtong Zhang, Tingyang Xu, and Ka-Chun Wong. Mdm: Molecular diffusion model for 3d molecule generation. *arXiv preprint arXiv:2209.05710*, 2022a.

Yinan Huang, Xingang Peng, Jianzhu Ma, and Muhan Zhang. 3dlinker: An e (3) equivariant variational autoencoder for molecular linker design. *arXiv preprint arXiv:2205.07309*, 2022b.

Fergus Imrie, Anthony R Bradley, Mihaela van der Schaar, and Charlotte M Deane. Deep generative models for 3d linker design. *Journal of chemical information and modeling*, 60(4):1983–1995, 2020.

John Ingraham, Vikas K Garg, Regina Barzilay, and Tommi Jaakkola. Generative models for graph-based protein design. 2019.

Wengong Jin, Jeremy Wohlwend, Regina Barzilay, and Tommi Jaakkola. Iterative refinement graph neural network for antibody sequence-structure co-design. *arXiv preprint arXiv:2110.04624*, 2021.

Bowen Jing, Stephan Eismann, Patricia Suriana, Raphael JL Townshend, and Ron Dror. Learning from protein structure with geometric vector perceptrons. *arXiv preprint arXiv:2009.01411*, 2020.

Bowen Jing, Gabriele Corso, Jeffrey Chang, Regina Barzilay, and Tommi Jaakkola. Torsional diffusion for molecular conformer generation. *arXiv preprint arXiv:2206.01729*, 2022.

John Jumper, Richard Evans, Alexander Pritzel, Tim Green, Michael Figurnov, Olaf Ronneberger, Kathryn Tunyasuvunakool, Russ Bates, Augustin Žídek, Anna Potapenko, et al. Highly accurate protein structure prediction with alphafold. *Nature*, 596(7873):583–589, 2021.

Zhifeng Kong, Wei Ping, Jiaji Huang, Kexin Zhao, and Bryan Catanzaro. Diffwave: A versatile diffusion model for audio synthesis. *arXiv preprint arXiv:2009.09761*, 2020.

Boqiao Lai, Jinbo Xu, et al. End-to-end deep structure generative model for protein design. *bioRxiv*, 2022.

Jin Sub Lee and Philip M Kim. Proteinsgm: Score-based generative modeling for de novo protein design. *bioRxiv*, 2022.

Junhyeok Lee and Seungu Han. Nu-wave: A diffusion probabilistic model for neural audio upsampling. *arXiv preprint arXiv:2104.02321*, 2021.

Xiang Lisa Li, John Thickstun, Ishaan Gulrajani, Percy Liang, and Tatsunori B Hashimoto. Diffusion-lm improves controllable text generation. *arXiv preprint arXiv:2205.14217*, 2022.

Zhixiu Li, Yuedong Yang, Eshel Faraggi, Jian Zhan, and Yaoqi Zhou. Direct prediction of profiles of sequences compatible with a protein structure by neural networks with fragment-based local and energy-based nonlocal profiles. *Proteins: Structure, Function, and Bioinformatics*, 82(10): 2565–2573, 2014.

Yeqing Lin and Mohammed AlQuraishi. Generating novel, designable, and diverse protein structures by equivariantly diffusing oriented residue clouds. *arXiv preprint arXiv:2301.12485*, 2023.

Jinglin Liu, Chengxi Li, Yi Ren, Feiyang Chen, and Zhou Zhao. Diffsinger: Singing voice synthesis via shallow diffusion mechanism. In *Proceedings of the AAAI Conference on Artificial Intelligence*, volume 36, pp. 11020–11028, 2022a.

Meng Liu, Youzhi Luo, Kanji Uchino, Koji Maruhashi, and Shuiwang Ji. Generating 3d molecules for target protein binding. *arXiv preprint arXiv:2204.09410*, 2022b.

Andreas Lugmayr, Martin Danelljan, Andres Romero, Fisher Yu, Radu Timofte, and Luc Van Gool. Repaint: Inpainting using denoising diffusion probabilistic models. In *Proceedings of the IEEE/CVF Conference on Computer Vision and Pattern Recognition*, pp. 11461–11471, 2022.

Shitong Luo, Yufeng Su, Xingang Peng, Sheng Wang, Jian Peng, and Jianzhu Ma. Antigen-specific antibody design and optimization with diffusion-based generative models for protein structures.

Shitong Luo, Chence Shi, Minkai Xu, and Jian Tang. Predicting molecular conformation via dynamic graph score matching. *Advances in Neural Information Processing Systems*, 34:19784–19795, 2021.

Shitong Luo, Jiaqi Guan, Jianzhu Ma, and Jian Peng. A 3d molecule generative model for structure-based drug design. *arXiv preprint arXiv:2203.10446*, 2022.

Youzhi Luo and Shuiwang Ji. An autoregressive flow model for 3d molecular geometry generation from scratch. In *International Conference on Learning Representations*, 2021.

Elman Mansimov, Omar Mahmood, Seokho Kang, and Kyunghyun Cho. Molecular geometry prediction using a deep generative graph neural network. *Scientific reports*, 9(1):1–13, 2019.

Sonja Müller-Späth, Andrea Soranno, Verena Hirschfeld, Hagen Hofmann, Stefan Rüegger, Luc Reymond, Daniel Nettels, and Benjamin Schuler. Charge interactions can dominate the dimensions of intrinsically disordered proteins. *Proceedings of the National Academy of Sciences*, 107(33): 14609–14614, 2010.

Vitali Nesterov, Mario Wieser, and Volker Roth. 3dmolnet: a generative network for molecular structures. *arXiv preprint arXiv:2010.06477*, 2020.

James O'Connell, Zhixiu Li, Jack Hanson, Rhys Heffernan, James Lyons, Kuldip Paliwal, Abdollah Dehzangi, Yuedong Yang, and Yaoqi Zhou. Spin2: Predicting sequence profiles from protein structures using deep neural networks. *Proteins: Structure, Function, and Bioinformatics*, 86(6): 629–633, 2018.

Sergey Ovchinnikov and Po-Ssu Huang. Structure-based protein design with deep learning. *Current opinion in chemical biology*, 65:136–144, 2021.

Robin Pearce and Yang Zhang. Deep learning techniques have significantly impacted protein structure prediction and protein design. *Current opinion in structural biology*, 68:194–207, 2021.

Xingang Peng, Shitong Luo, Jiaqi Guan, Qi Xie, Jian Peng, and Jianzhu Ma. Pocket2mol: Efficient molecular sampling based on 3d protein pockets. *arXiv preprint arXiv:2205.07249*, 2022.

Yifei Qi and John ZH Zhang. Densecpd: improving the accuracy of neural-network-based computational protein sequence design with densenet. *Journal of chemical information and modeling*, 60 (3):1245–1252, 2020.

Matthew Ragoza, Tomohide Masuda, and David Ryan Koes. Generating 3D molecules conditional on receptor binding sites with deep generative models. *Chem Sci*, 13:2701–2713, Feb 2022. doi: 10.1039/D1SC05976A.

Sari Sabban and Mikhail Markovsky. Ramanet: Computational de novo helical protein backbone design using a long short-term memory generative neural network. *bioRxiv*, pp. 671552, 2020.

Chence Shi, Shitong Luo, Minkai Xu, and Jian Tang. Learning gradient fields for molecular conformation generation. In *International Conference on Machine Learning*, pp. 9558–9568. PMLR, 2021.

Gregor Simm, Robert Pinsler, and José Miguel Hernández-Lobato. Reinforcement learning for molecular design guided by quantum mechanics. In *International Conference on Machine Learning*, pp. 8959–8969. PMLR, 2020a.

Gregor N. C. Simm, José Miguel Hernández-Lobato, XXX, and XXX. A generative model for molecular distance geometry. In *Proceedings of the 37th International Conference on Machine Learning*, ICML'20. JMLR.org, 2020b.

Jascha Sohl-Dickstein, Eric Weiss, Niru Maheswaranathan, and Surya Ganguli. Deep unsupervised learning using nonequilibrium thermodynamics. In *International Conference on Machine Learning*, pp. 2256–2265. PMLR, 2015.

Yang Song, Jascha Sohl-Dickstein, Diederik P Kingma, Abhishek Kumar, Stefano Ermon, and Ben Poole. Score-based generative modeling through stochastic differential equations. *arXiv preprint arXiv:2011.13456*, 2020.

Velin Z Spassov, Lisa Yan, and Paul K Flook. The dominant role of side-chain backbone interactions in structural realization of amino acid code. chirotor: A side-chain prediction algorithm based on side-chain backbone interactions. *Protein Science*, 16(3):494–506, 2007.

Alexey Strokach and Philip M Kim. Deep generative modeling for protein design. *Current opinion in structural biology*, 72:226–236, 2022.

Alexey Strokach, David Becerra, Carles Corbi-Verge, Albert Perez-Riba, and Philip M Kim. Fast and flexible protein design using deep graph neural networks. *Cell Systems*, 11(4):402–411, 2020.

Cheng Tan, Zhangyang Gao, Jun Xia, and Stan Z Li. Generative de novo protein design with global context. *arXiv preprint arXiv:2204.10673*, 2022.

Doug Tischer, Sidney Lisanza, Jue Wang, Runze Dong, Ivan Anishchenko, Lukas F Milles, Sergey Ovchinnikov, and David Baker. Design of proteins presenting discontinuous functional sites using deep learning. *Biorxiv*, 2020.

Brian L Trippe, Jason Yim, Doug Tischer, Tamara Broderick, David Baker, Regina Barzilay, and Tommi Jaakkola. Diffusion probabilistic modeling of protein backbones in 3d for the motif-scaffolding problem. *arXiv preprint arXiv:2206.04119*, 2022.

Jingxue Wang, Huali Cao, John ZH Zhang, and Yifei Qi. Computational protein design with deep learning neural networks. *Scientific reports*, 8(1):1–9, 2018.

Jue Wang, Sidney Lisanza, David Juergens, Doug Tischer, Joseph L Watson, Karla M Castro, Robert Ragotte, Amijai Saragovi, Lukas F Milles, Minkyung Baek, et al. Scaffolding protein functional sites using deep learning. *Science*, 377(6604):387–394, 2022a.

Wujie Wang, Minkai Xu, Chen Cai, Benjamin Kurt Miller, Tess Smidt, Yusu Wang, Jian Tang, and Rafael Gómez-Bombarelli. Generative coarse-graining of molecular conformations. *arXiv preprint arXiv:2201.12176*, 2022b.

Joseph L Watson, David Juergens, Nathaniel R Bennett, Brian L Trippe, Jason Yim, Helen E Eisenach, Woody Ahern, Andrew J Borst, Robert J Ragotte, Lukas F Milles, et al. De novo design of protein structure and function with rfdiffusion. *Nature*, pp. 1–3, 2023.

Jay Whang, Mauricio Delbracio, Hossein Talebi, Chitwan Saharia, Alexandros G Dimakis, and Peyman Milanfar. Deblurring via stochastic refinement. In *Proceedings of the IEEE/CVF Conference on Computer Vision and Pattern Recognition*, pp. 16293–16303, 2022.

Julia Wolleb, Robin Sandkühler, Florentin Bieder, Philippe Valmaggia, and Philippe C Cattin. Diffusion models for implicit image segmentation ensembles. In *International Conference on Medical Imaging with Deep Learning*, pp. 1336–1348. PMLR, 2022.

Kevin E Wu, Kevin K Yang, Rianne van den Berg, James Y Zou, Alex X Lu, and Ava P Amini. Protein structure generation via folding diffusion. *arXiv preprint arXiv:2209.15611*, 2022a.

Lemeng Wu, Chengyue Gong, Xingchao Liu, Mao Ye, and Qiang Liu. Diffusion-based molecule generation with informative prior bridges. *arXiv preprint arXiv:2209.00865*, 2022b.

Zachary Wu, Kadina E Johnston, Frances H Arnold, and Kevin K Yang. Protein sequence design with deep generative models. *Current opinion in chemical biology*, 65:18–27, 2021.

Minkai Xu, Shitong Luo, Yoshua Bengio, Jian Peng, and Jian Tang. Learning neural generative dynamics for molecular conformation generation. In *International Conference on Learning Representations*, 2020.

Minkai Xu, Wujie Wang, Shitong Luo, Chence Shi, Yoshua Bengio, Rafael Gomez-Bombarelli, and Jian Tang. An end-to-end framework for molecular conformation generation via bilevel programming. In *International Conference on Machine Learning*, pp. 11537–11547. PMLR, 2021.

Minkai Xu, Lantao Yu, Yang Song, Chence Shi, Stefano Ermon, and Jian Tang. Geodiff: A geometric diffusion model for molecular conformation generation. *arXiv preprint arXiv:2203.02923*, 2022.

Jason Yim, Brian L Trippe, Valentin De Bortoli, Emile Mathieu, Arnaud Doucet, Regina Barzilay, and Tommi Jaakkola. Se (3) diffusion model with application to protein backbone generation. *arXiv preprint arXiv:2302.02277*, 2023.

Yuan Zhang, Yang Chen, Chenran Wang, Chun-Chao Lo, Xiuwen Liu, Wei Wu, and Jinfeng Zhang. Prodconn: Protein design using a convolutional neural network. *Proteins: Structure, Function, and Bioinformatics*, 88(7):819–829, 2020.

Jinhua Zhu, Yingce Xia, Chang Liu, Lijun Wu, Shufang Xie, Tong Wang, Yusong Wang, Wengang Zhou, Tao Qin, Houqiang Li, et al. Direct molecular conformation generation. *arXiv preprint arXiv:2202.01356*, 2022.